control keratinocytes did not (Fig. 5A). In addition, FRP1-positive cells were detected in SJS/TEN lesions, whereas no FRP1-positive cells were detected in the nonlesional skin of SJS/TEN, ODSR lesions, or normal skin (Fig. 5B). Abundant annexin A1 was also detected in the SJS/TEN lesions; in contrast, little annexin A1 was seen in the nonlesional skin of SJS/TEN, in ODSR lesions, or in normal skin (Fig. 5C). When SJS/TEN keratinocytes were exposed to *N*-formyl-Met-Leu-Phe (*f*MLP), which is an FPR1 ligand, they showed a cytotoxic response, whereas no effects were seen in healthy control keratinocytes (Fig. 6A). Moreover, Nec-1 effectively inhibited *f*MLP-induced SJS/TEN keratinocyte death. A neutralizing antibody against FPR1 prevented SJS/TEN supernatant–induced cytotoxicity (Fig. 6B). *f*MLP induced cytotoxicity in SJS/TEN keratinocytes in a dose-dependent manner (Fig. 6C). FPR2 is also a receptor for annexin A1 (*22*), but when we added an FPR2 antagonist (WRW4) (Trp-Arg-Trp-Trp-Trp-Trp) (0.1 or 1.0 μM) during SJS/TEN supernatant–induced cytotoxicity, cytotoxicity was not inhibited (Fig. 6D).

FPR1 has not previously been known to relate to both apoptosis and necroptosis. To show that the FPR1 signal stimulates a necroptosis pathway, we analyzed the RIP1/RIP3 immunocomplex obtained from a Flag-tagged RIP3 pull-down in Flag-RIP3-HeLa cells. We

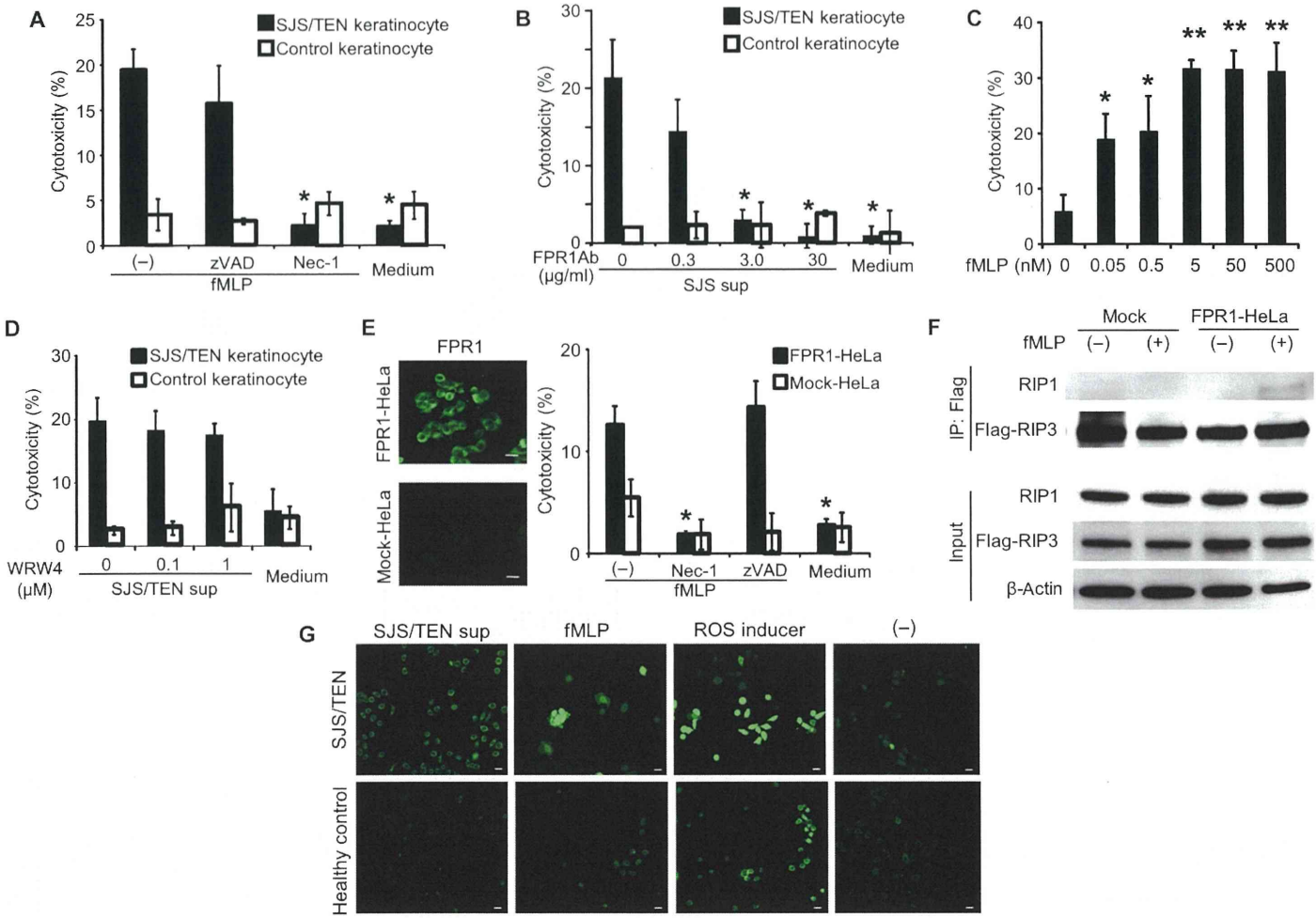

Fig. 6. FRP1 activation induces necrosis via the RIP1/RIP3 complex. (**A**) Effect of *f*MLP (5 nM) on cytotoxicity in the presence of zVAD (50 μM) or Nec-1 (50 μM) was analyzed using keratinocytes from SJS/TEN patients or healthy controls ($n = 4$). *$P < 0.05$. Keratinocytes were obtained from patient no. 10 (postlesional skin) and healthy control no. 5. (**B**) Effect of FPR1 neutralizing antibody on SJS/TEN PBMC supernatant–induced cytotoxicity was analyzed ($n = 4$). *$P < 0.01$. Keratinocytes were obtained from patient no. 10 and healthy control no. 5. PBMCs were obtained from patient no. 3 (postlesional skin). (**C**) Dose dependence of cytotoxicity by *f*MLP ($n = 4$). *$P < 0.05$; **$P < 0.01$. Keratinocytes were obtained from patient no. 3 (postlesional skin). (**D**) Effect of FPR2 antagonist (WRW4) on SJS/TEN PBMC supernatant cytotoxicity. Keratinocytes were preincubated with WRW4 for 15 min before exposure to SJS/TEN supernatant ($n = 5$). Keratinocytes were obtained from patient no. 10 (postlesional skin) and healthy control no. 7. PBMCs were obtained from patient no. 3 ($n = 4$). (**E**) Effect of necrosis and apoptosis inhibitors on cytotoxicity in FPR1-transfected, Flag-RIP3–expressing HeLa cells. Flag-RIP3–expressing HeLa cells were stably transfected with FPR1 and stimulated with *f*MLP, and cytotoxicity was assessed ($n = 4$). *$P < 0.01$ versus *f*MLP. (**F**) Immunoprecipitation of a Flag-tagged RIP3 pull-down from *f*MLP-exposed HeLa cells (FPR1-HeLa cells or mock-transfected HeLa cells). The experiments were repeated three times, and representative data are shown. (**G**) Representative images showing sensitivity of SJS/TEN keratinocytes to FPR1-induced ROS generation. SJS/TEN sup (25%), *f*MLP (500 nM), or ROS inducer (pyocyanin) (200 μM) was added to keratinocytes from SJS/TEN patients or healthy controls. After 30 min, ROS generation was measured. Scale bars, 5 μm. Keratinocytes were obtained from patient no. 3 (postlesional skin) and healthy control no. 6.

found that *f*MLP stimulation induced cytotoxicity only in FPR1-expressing RIP3-HeLa cells and not in mock-transfected cells (Fig. 6E). Although zVAD did not inhibit cytotoxicity, Nec-1 completely inhibited the effect. With *f*MLP stimulation, the RIP1/RIP3 complex was detected only in FRP1-expressing HeLa cells and not in mock-transfected HeLa cells (Fig. 5F). These data point to the conclusion that annexin A1 in the SJS/TEN supernatant is a potent activator of FPR1 and induces necroptosis in SJS/TEN keratinocytes.

The FPR1 signal induces the generation of reactive oxygen species (ROS) (*23*), which is also a mediator of necroptosis (*18*). Therefore, we investigated ROS generation in SJS/TEN supernatant–exposed keratinocytes. High levels of ROS generation were observed in SJS/TEN supernatant–exposed or *f*MLP-treated SJS/TEN keratinocytes examined by fluorescence microscopy, but not in control keratinocytes (Fig. 6G), indicating that SJS/TEN keratinocytes are sensitive to FPR1-induced ROS generation. Because FPR1 activates the MAP kinase cascade (*21*), we assessed the activation of MAP kinase in FPR1-expressing HeLa and mock-transfected HeLa cells. *f*MLP exposure did not induce the phosphorylation of c-Jun N-terminal kinase (JNK), p38, or ERK (extracellular signal–regulated kinase) (fig. S8).

Therapy for SJS/TEN model mice by necroptosis inhibitor

We administered a necroptosis blocker to our SJS/TEN model mice. NSA, which blocks necroptosis by inhibiting MLKL (*17*), prevents SJS/TEN supernatant–induced cytotoxicity in vitro (Fig. 7A). Whereas the vehicle-treated model mice showed marked conjunctival congestion and abundant cell death in their conjunctival epithelium, the NSA-treated mice showed no such reactions (Fig. 7B). We found numerous dead epithelial cells in the vehicle-treated model mice but not in the NSA-treated model mice (Fig. 7, C and D). Moreover, the vehicle-treated model mice showed RIP3 and FPR1 in conjunctiva similar to those seen in human SJS/TEN (Figs. 2D and 4E), whereas the NSA-treated model mice did not show these proteins in their conjunctiva (Fig. 7D).

DISCUSSION

Here, we show that necroptosis can be triggered by the interaction of annexin A1 and FPR1 and may contribute to the pathogenesis of SJS/TEN. Our data suggest that causative drug exposure induces annexin A1 secretion from monocytes in SJS/TEN patients. Annexin

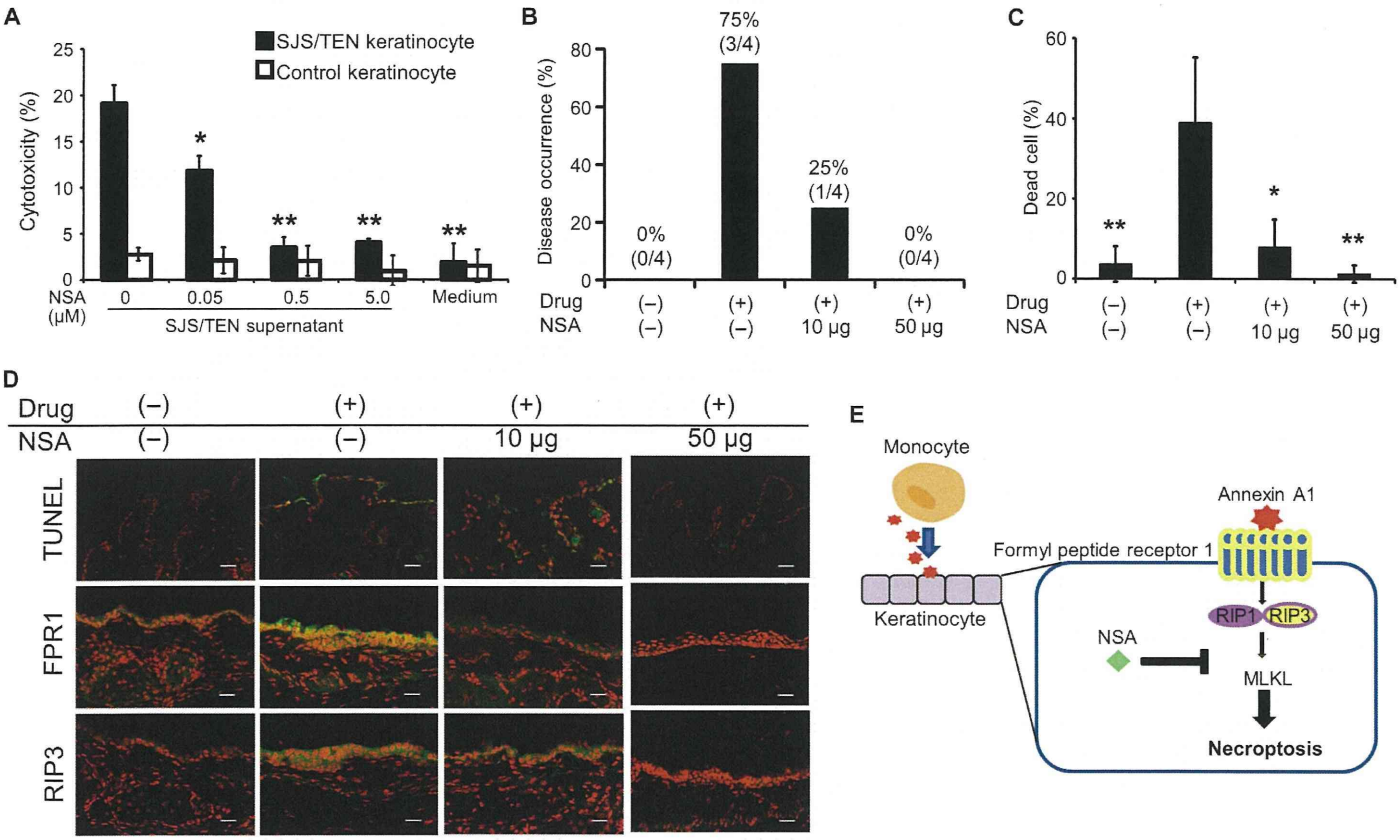

Fig. 7. Inhibition of necroptosis prevents SJS/TEN in model mice. (**A**) Effect of NSA on SJS/TEN supernatant–induced cytotoxicity ($n = 4$). *$P < 0.05$; **$P < 0.01$. Keratinocytes and PBMCs were obtained from patient no. 3 (postlesional skin). Keratinocytes were obtained from healthy control no. 4. (**B**) Model mice received NSA intraperitoneally, and eye abnormalities were scored as disease occurrence ($n = 4$). (**C**) Percentage of dead cells in conjunctiva epithelia was calculated ($n = 4$). *$P < 0.05$; **$P < 0.01$ versus Drug (+), NSA (–). (**D**) Using TUNEL (terminal deoxynucleotidyl transferase–mediated deoxyuridine triphosphate nick end labeling) assay, dead cells were visualized, and RIP3 and FPR1 expression was imaged in the conjunctiva of model mice. Nuclei were stained with PI. Representative images are shown. Scale bars, 10 μm. (**E**) Scheme of keratinocyte death mechanism. In SJS/TEN, the causative drug stimulates PBMCs (monocytes) to secrete annexin A1 (yellow star). The released annexin A1 binds to FPR1 and activates the necroptosis pathway through the RIP1/RIP3 complex. NSA, an MLKL inhibitor, can block necroptosis.

A1 in turn binds to FPR1 and induces FPR1 expression in keratinocytes, resulting in cell death via a necroptosis pathway (Fig. 7E).

Several stimulators of necroptosis, such as Fas and TNF-α, also stimulate apoptosis (*24*). Although it has been shown that artificial inhibition of casapse-8 or overexpression of RIP3 tends to induce necroptosis (*16*, *25*), it was not known whether these imbalances also occur naturally. Our present data show that necroptosis signaling by annexin A1/FRP1 does not appear to overlap with apoptosis. To induce keratinocyte necroptosis, both annexin A1 and FPR1 are required. We show that annexin A1 induces FPR1 expression in SJS/TEN keratinocytes. Therefore, keratinocyte necroptosis may occur only when annexin A1 is up-regulated, namely, under conditions of drug allergy.

Several mediators of SJS/TEN have been proposed, such as Fas ligand (*5*), soluble Fas ligand (*26*), perforin, granzyme B (*27*), and granulysin (*2*, *28*). For example, granulysin was identified by DNA microarray of SJS/TEN bullae cells; the data showed the mRNA of granulysin to be elevated, as well as the mRNAs of other proapoptotic molecules, such as FasL, perforin, and granzyme B (*2*). These results suggest that several pathways are activated in apoptosis in vivo.

It is not clear why these "cell death mediators" affect skin and result in widespread mucocutaneous erosions in SJS/TEN but not in ODSR, and whether there are individual differences in proapoptotic molecule expression is unknown. In this regard, inducible FPR1 expression levels differ greatly between SJS/TEN and ODSR (Fig. 5, A and B), suggesting that inducible FPR1 expression levels may determine SJS/TEN or ODSR occurrence and regulate the necroptosis that is seen in SJS/TEN.

Although there are no genetic differences in FPR1 promoters among SJS/TEN patients, ODSR patients, and healthy controls (data file S1), annexin A1–FRP1 are candidate markers of disease occurrence and may be promising therapeutic targets. In addition, necroptosis is a potential drug target for SJS/TEN treatment, and NSA is a therapeutic candidate.

MATERIALS AND METHODS

Study design

For the human sample studies, skin PBMCs and sera from healthy controls and SJS/TEN or ODSRs patients (table S2) were obtained from Hokkaido University Hospital. The collection of samples was approved by the local ethics committee and the institutional review board of Hokkaido University. To investigate SJS/TEN pathogenesis, approval was given for the collection of blood, serum, and skin samples. We also explained the potential side effects of skin biopsy to the patients. After we obtained the informed consent of the patient, we obtained the blood, serum, and skin samples in the acute phase of the disease and in the resolution phase.

The mouse studies were performed under a protocol approved by the ethical committee for animal studies of Hokkaido University. Immunocompromised NOG mice at 6 to 7 weeks of age were purchased from Jackson Laboratory.

Immunohistochemistry

The following primary antibodies were used: RIP3 (Abcam) and FPR1 (LifeSpan). Anti–annexin A1 antibody was generated by peptide immunization of rabbits, as was rabbit polyclonal antibody to the synthetic peptide MAMVSEFLKQAWF, corresponding to amino acid residues 1 to 13 in annexin A1. These antibodies were generated at our request by Hokudo Co. Ltd.

Electron microscopy

Skin sections were fixed by the dropwise addition of glutaraldehyde and were analyzed according to standard methods. Necrotic and apoptotic cells were counted in all keratinocytes (N = 80) in the SJS/TEN lesions.

The morphological changes in supernatant-treated keratinocytes by electron microscopy were examined. Necrotic and apoptotic cells were counted among dead keratinocytes (n = 35).

ELISPOT IFN-γ assay

PBMCs were prepared from patients' blood and isolated by Ficoll-Isopaque (Pharmacia Fine Chemicals) density gradient centrifugation. The number of IFN-γ–producing cells was determined with an ELISPOT assay kit (Human IFN-γ ELISPOT PVDF-Enzymatic; Diaclone). The number of spots was counted under a dissecting microscope (SMZ1500; Nikon).

Supernatant

PBMCs were obtained from SJS/TEN or ODSRs patients. $CD14^+$ and $CD8^+$ cell depletions were performed with magnetic-activated cell sorting (MACS; Miltenyi Biotec). Isolated cells were exposed to causative drugs and then cultured for 5 days to allow proliferation of drug-specific T cells. The cells were stimulated by reexposure with same causative drugs for 1 day, and then supernatant was collected. Drug concentration was determined from the data of a lymphocyte transformation test (*29*). In some experiments, PBMCs were incubated with several concentrations of causative drug for 5 days. [^{3}H]Thymidine (1 μCi) was added for the last 12 hours. Causative drug–specific proliferation was determined by measuring [^{3}H]thymidine incorporation. The results were expressed as stimulation indices (SI): (cpm in cultures + drug)/(cpm in cultures without drug). The concentration with the highest SI was chosen for further experiments.

Keratinocyte culture

Primary keratinocytes were isolated from patients, cultured and then expanded in CnT-57 from CELLnTEC, and used for the assay with no more than four passages. The keratinocytes were incubated with CnT-57 in a 5% CO_2 incubator at 37°C.

Cytotoxic assays

Cultured keratinocytes were added to the supernatant of the causative drug–exposed PBMCs. In some experiments, zVAD (R&D Systems) or Nec-1 (Enzo Life Sciences) was preincubated with the cells for 1 hour before supernatant addition. *f*MLP and Ac2-26 were purchased from Sigma-Aldrich. Anti–MHC I antibody (W6/32) was purchased from BioLegend. FPR2 antagonist (WRW4) was purchased from Tocris Bioscience. At 8 or 16 hours, the cytotoxicity was analyzed with an LDH (lactate dehydrogenase) assay (R&D Systems) and/or trypan blue staining (R&D Systems). The data were comparable with LDH or trypan blue staining assays (fig. S9). All experiments were repeated at least three times.

siRNA transfection

For transient knockdown, keratinocytes were transfected on two consecutive days with nontargeting RNA duplexes or duplexes targeting RIP3 (siRNA-1: GAACUGUUUGUUAACGCAA and siRNA-2: GGCAAGUCUGGAUAACGA), and control siRNA duplex (that is, a scrambled siRNA with a sequence that matched no known mRNA sequence in the vertebrate genome) (Ambion) using Lipofectamine RNAiMAX (Invitrogen). At 48 hours, cells were used in experiments.

Mass spectrometry (LC-MS/MS)

The proteins in SJS/TEN supernatant were identified by mass spectrometry analysis as described (*30*). The primary ion spectrum data generated by LC-MS/MS were screened against International Protein Index human protein databases with the Mascot program (Matrix Science) to identify high-scoring proteins.

Removal of annexin A1 from supernatant

Supernatant was mixed with the anti–annexin A1 antibody and gently mixed at 4°C overnight. Protein G Dynabeads (Dynal) were then added to the mixture, followed by 2 hours of rotation at 4°C. Annexin A1 could not be detected in annexin A1–depleted SJS/TEN supernatant with annexin A1 peptide ELISA.

Annexin A1 peptide ELISA

Rabbit polyclonal antibody against annexin A1 peptide (amino acids 1 to 13) was used for annexin A1 peptide ELISA to measure annexin A1 concentration.

Samples were added to the wells of a microplate. After overnight incubation at 4°C, rabbit polyclonal antibody against annexin A1 peptide (amino acids 1 to 13) (1: 5000) was added, followed by β-galactosidase anti-rabbit IgG antibody (1:2000). The fluorescence was measured with a microplate reader.

FPR1-expressing stable cell lines

3xFlag-RIP3-HeLa cells were established as described (*17*). Normal human full-length FRP1 cDNA (complementary DNA) was synthesized by Integrated DNA Technologies Inc. and subcloned into the Xho I and Kpn I sites of pcDNA3.1/Zeo vector (Invitrogen). RIP3-HeLa cells were transfected with pcDNA3.1/Zeo plasmid encoding FRP1 with FuGENE 6 (Roche) and were selected with Zeocin (100 μg/ml) (Invitrogen).

Immunoprecipitation

The cells were lysed for 30 min on ice in a lysis buffer. Cell lysate was spun at 15,000 rpm for 10 min, and the soluble fraction was collected. One milligram of extracted protein in lysis buffer was immunoprecipitated for 2 hours with anti-FLAG M2 affinity gel (Sigma-Aldrich) at 4°C. The immunoprecipitates were washed five times with lysis buffer. The beads were eluted with the corresponding antigenic peptide (250 μg/ml).

FPR1-induced ROS generation

SJS/TEN supernatant (25%), *f*MLP (500 nM), or ROS inducer (pyocyanin) (200 μM) was added to keratinocytes from SJS/TEN patients or healthy controls. After 30 min, ROS generation was detected by using the Total ROS Detection Kit (Enzo Life Sciences).

Treatment of necroptosis inhibitor for SJS/TEN model mice

Patient PBMCs (2×10^6) were injected intravenously into immunocompromised NOG mice, followed by oral administration of a causative drug for 12 days (*15*). NSA (10 or 50 μg) (provided by L. Sun and X. Wang) or DMSO was also administered intraperitoneally to mice daily. The mice were observed for manifestations of eye disease.

Terminal deoxynucleotidyl transferase–mediated deoxyuridine triphosphate nick end labeling

To detect dead cells by DNA fragmentation by labeling the terminal end of nucleic acids, a TUNEL assay was performed according to the manufacturer's protocol (Takara Bio).

Statistics

In all figures, data are presented as means ± SD of at least three independent experiments. *P* values were calculated with one-way analysis of variance (ANOVA) and two-tailed independent Student's *t* tests, and $P < 0.05$ was considered significant.

SUPPLEMENTARY MATERIALS

www.sciencetranslationalmedicine.org/cgi/content/full/6/245/245ra95/DC1

Fig. S1. Causative drug–specific lymphocytes in patients' peripheral blood.
Fig. S2. The cytotoxicity of supernatant from DIHS/DRESS PBMCs.
Fig. S3. The cytotoxicity of supernatant from irrelevant drug–exposed SJS/TEN PBMCs.
Fig. S4. The cytotoxicity of keratinocytes from normal-appearing postlesional skin and nonlesional skin.
Fig. S5. Protein levels of necroptosis signaling molecules in keratinocytes from SJS/TEN patients, ODSR patients, or healthy controls.
Fig. S6. Effect of poly(I:C), TNF-α, and granulysin on SJS/TEN keratinocyte cytotoxicity.
Fig. S7. The cytotoxicity of $CD14^{bright}$ $CD16^{-}$ and $CD14^{dim}$ $CD16^{+}$ cells on SJS/TEN keratinocytes.
Fig. S8. FPR1 stimulation does not induce phosphorylation of JNK, p38, or ERK.
Fig. S9. Cytotoxicity in SJS/TEN keratinocytes, ODSR keratinocytes, or healthy control keratinocytes induced by PBMC supernatant, as measured by LDH assay.
Table S1. Mass spectrometry result of the proteins in SJS/TEN supernatant.
Table S2. Patient and healthy control information.
Data File S1. The promoter region of FPR1 has no pathogenic mutations.
Reference (*31*)

REFERENCES AND NOTES

1. A. Downey, C. Jackson, N. Harun, A. Cooper, Toxic epidermal necrolysis: Review of pathogenesis and management. *J. Am. Acad. Dermatol.* **66**, 995–1003 (2012).
2. W.H. Chung, S. I. Hung, J. Y. Yang, S. C. Su, S. P. Huang, C. Y. Wei, S. W. Chin, C. C. Chiou, S. C. Chu, H. C. Ho, C. H. Yang, C. F. Lu, J. Y. Wu, Y. D. Liao, Y. T. Chen, Granulysin is a key mediator for disseminated keratinocyte death in Stevens-Johnson syndrome and toxic epidermal necrolysis. *Nat. Med.* **14**, 1343–1350 (2008).
3. T. Hanafusa, H. Azukizawa, S. Matsumura, I. Katayama, The predominant drug-specific T-cell population may switch from cytotoxic T cells to regulatory T cells during the course of anticonvulsant-induced hypersensitivity. *J. Dermatol. Sci.* **65**, 213–219 (2012).
4. W. H. Chung, S. I. Hung, Recent advances in the genetics and immunology of Stevens-Johnson syndrome and toxic epidermal necrosis. *J. Dermatol. Sci.* **66**, 190–196 (2012).
5. I. Viard, P. Wehrli, R. Bullani, P. Schneider, N. Holler, D. Salomon, T. Hunziker, J. H. Saurat, J. Tschopp, L. E. French, Inhibition of toxic epidermal necrolysis by blockade of CD95 with human intravenous immunoglobulin. *Science* **282**, 490–493 (1998).
6. P. Golstein, G. Kroemer, Cell death by necrosis: Towards a molecular definition. *Trends Biochem. Sci.* **32**, 37–43 (2007).
7. A. Kawahara, T. Kobayashi, S. Nagata, Inhibition of Fas-induced apoptosis by Bcl-2. *Oncogene* **17**, 2549–2554 (1998).
8. D. Vercammen, P. Vandenabeele, R. Beyaert, W. Declercq, W. Fiers, Tumour necrosis factor-induced necrosis versus anti-Fas-induced apoptosis in L929 cells. *Cytokine* **9**, 801–808 (1997).
9. A. Degterev, Z. Huang, M. Boyce, Y. Li, P. Jagtap, N. Mizushima, G. D. Cuny, T. J. Mitchison, M. A. Moskowitz, J. Yuan, Chemical inhibitor of nonapoptotic cell death with therapeutic potential for ischemic brain injury. *Nat. Chem. Biol.* **1**, 112–119 (2005).
10. A. Degterev, J. Hitomi, M. Germscheid, I. L. Ch'en, O. Korkina, X. Teng, D. Abbott, G. D. Cuny, C. Yuan, G. Wagner, S. M. Hedrick, S. A. Gerber, A. Lugovskoy, J. Yuan, Identification of RIP1 kinase as a specific cellular target of necrostatins. *Nat. Chem. Biol.* **4**, 313–321 (2008).
11. P. S. Welz, A. Wullaert, K. Vlantis, V. Kondylis, V. Fernández-Majada, M. Ermolaeva, P. Kirsch, A. Sterner-Kock, G. van Loo, M. Pasparakis, FADD prevents RIP3-mediated epithelial cell necrosis and chronic intestinal inflammation. *Nature* **477**, 330–334 (2011).
12. C. Günther, E. Martini, N. Wittkopf, K. Amann, B. Weigmann, H. Neumann, M. J. Waldner, S. M. Hedrick, S. Tenzer, M. F. Neurath, C. Becker, Caspase-8 regulates TNF-α-induced epithelial necroptosis and terminal ileitis. *Nature* **477**, 335–339 (2011).
13. A. Beeler, O. Engler, B. O. Gerber, W. J. Pichler, Long-lasting reactivity and high frequency of drug-specific T cells after severe systemic drug hypersensitivity reactions. *J. Allergy Clin. Immunol.* **117**, 455–462 (2006).
14. A. Rozieres, A. Hennino, K. Rodet, M. C. Gutowski, N. Gunera-Saad, F. Berard, G. Cozon, J. Bienvenu, J. F. Nicolas, Detection and quantification of drug-specific T cells in penicillin allergy. *Allergy* **64**, 534–542 (2009).

15. N. Saito, N. Yoshioka, R. Abe, H. Qiao, Y. Fujita, D. Hoshina, A. Suto, S. Kase, N. Kitaichi, M. Ozaki, H. Shimizu, Stevens-Johnson syndrome/toxic epidermal necrolysis mouse model generated by using PBMCs and the skin of patients. *J. Allergy Clin. Immunol.* **131**, 434–441.e9 (2013).
16. D. W. Zhang, J. Shao, J. Lin, N. Zhang, B. J. Lu, S. C. Lin, M. Q. Dong, J. Han, RIP3, an energy metabolism regulator that switches TNF-induced cell death from apoptosis to necrosis. *Science* **325**, 332–336 (2009).
17. L. Sun, H. Wang, Z. Wang, S. He, S. Chen, D. Liao, L. Wang, J. Yan, W. Liu, X. Lei, X. Wang, Mixed lineage kinase domain-like protein mediates necrosis signaling downstream of RIP3 kinase. *Cell* **148**, 213–227 (2012).
18. Z. Wang, H. Jiang, S. Chen, F. Du, X. Wang, The mitochondrial phosphatase PGAM5 functions at the convergence point of multiple necrotic death pathways. *Cell* **148**, 228–243 (2012).
19. M. Perretti, F. D'Acquisto, Annexin A1 and glucocorticoids as effectors of the resolution of inflammation. *Nat. Rev. Immunol.* **9**, 62–70 (2009).
20. M. Tohyama, H. Watanabe, S. Murakami, Y. Shirakata, K. Sayama, M. Iijima, K. Hashimoto, Possible involvement of CD14+ CD16+ monocyte lineage cells in the epidermal damage of Stevens–Johnson syndrome and toxic epidermal necrolysis. *Br. J. Dermatol.* **166**, 322–330 (2012).
21. S. D. Kim, J. M. Kim, S. H. Jo, H. Y. Lee, S. Y. Lee, J. W. Shim, S. K. Seo, J. Yun, Y. S. Bae, Functional expression of formyl peptide receptor family in human NK cells. *J. Immunol.* **183**, 5511–5517 (2009).
22. G. Leoni, A. Alam, P. A. Neumann, J. D. Lambeth, G. Cheng, J. McCoy, R. S. Hilgarth, K. Kundu, N. Murthy, D. Kusters, C. Reutelingsperger, M. Perretti, C. A. Parkos, A. S. Neish, A. Nusrat, Annexin A1, formyl peptide receptor, and NOX1 orchestrate epithelial repair. *J. Clin. Invest.* **123**, 443–454 (2013).
23. C. C. Wentworth, A. Alam, R. M. Jones, A. Nusrat, A. S. Neish, Enteric commensal bacteria induce extracellular signal-regulated kinase pathway signaling via formyl peptide receptor-dependent redox modulation of dual specific phosphatase 3. *J. Biol. Chem.* **286**, 38448–38455 (2011).
24. P. Vandenabeele, L. Galluzzi, T. Vanden Berghe, G. Kroemer, Molecular mechanisms of necroptosis: An ordered cellular explosion. *Nat. Rev. Mol. Cell Biol.* **11**, 700–714 (2010).
25. M. A. O'Donnell, E. Perez-Jimenez, A. Oberst, A. Ng, R. Massoumi, R. Xavier, D. R. Green, A. T. Ting, Caspase 8 inhibits programmed necrosis by processing CYLD. *Nat. Cell Biol.* **13**, 1437–1442 (2011).
26. R. Abe, T. Shimizu, A. Shibaki, H. Nakamura, H. Watanabe, H. Shimizu, Toxic epidermal necrolysis and Stevens-Johnson syndrome are induced by soluble Fas ligand. *Am. J. Pathol.* **162**, 1515–1520 (2003).
27. S. J. Posadas, A. Padial, M. J. Torres, C. Mayorga, L. Leyva, E. Sanchez, J. Alvarez, A. Romano, C. Juarez, M. Blanca, Delayed reactions to drugs show levels of perforin, granzyme B, and Fas-L to be related to disease severity. *J. Allergy Clin. Immunol.* **109**, 155–161 (2002).
28. R. Abe, N. Yoshioka, J. Murata, Y. Fujita, H. Shimizu, Granulysin as a marker for early diagnosis of the Stevens–Johnson syndrome. *Ann. Intern. Med.* **151**, 514–515 (2009).
29. G. Porebski, T. Pecaric-Petkovic, M. Groux-Keller, M. Bosak, T. T. Kawabata, W. J. Pichler, In vitro drug causality assessment in Stevens–Johnson syndrome—Alternatives for lymphocyte transformation test. *Clin. Exp. Allergy* **43**, 1027–1037 (2013).
30. R. S. Nozawa, K. Nagao, H. T. Masuda, O. Iwasaki, T. Hirota, N. Nozaki, H. Kimura, C. Obuse, Human POGZ modulates dissociation of HP1α from mitotic chromosome arms through Aurora B activation. *Nat. Cell Biol.* **12**, 719–727 (2010).
31. H. M. Miettinen, Regulation of human formyl peptide receptor 1 synthesis: Role of single nucleotide polymorphisms, transcription factors, and inflammatory mediators. *PLOS One* **6**, e28712 (2011).

Acknowledgments: We thank. M. Kagaya-Takehara and A. Moriya for their technical expertise, and H. Takahashi and S. Hatakeyama for their technical advice. Flag-RIP3-HeLa cells were donated by L. Sun and X. Wang. **Funding:** This work was supported in part by a Health and Labor Sciences Research Grant from the Ministry of Health, Labor, and Welfare of Japan (Research on Development of New Drugs; H24-Bio-001 to R.A.) and a Grant-in-Aid for Scientific Research from the Ministry of Education, Culture, Sports, Science and Technology of Japan (no. 24390275 to R.A.). **Author contributions:** N.S. conceived the study, designed the experiments, wrote the paper, and performed most of the experiments with help from H.Q., T.Y., K. Nishimura, A.S., Y.F., and H.N.; R.A. conceived the study, designed the experiments, and wrote the paper; H.S. analyzed results and wrote the paper; S. Shinkuma generated FRP1-expressing HeLa cells; S. Suzuki and T.N. performed the mutation search in the FPR1 promoter region; and K. Nagao and C.O. performed mass spectrometry (LC-MS/MS). **Competing interests:** The authors declare that they have no competing interests.

Submitted 10 December 2013
Accepted 27 May 2014
Published 16 July 2014
10.1126/scitranslmed.3008227

Citation: N. Saito, H. Qiao, T. Yanagi, S. Shinkuma, K. Nishimura, A. Suto, Y. Fujita, S. Suzuki, T. Nomura, H. Nakamura, K. Nagao, C. Obuse, H. Shimizu, R. Abe, An annexin A1–FPR1 interaction contributes to necroptosis of keratinocytes in severe cutaneous adverse drug reactions. *Sci. Transl. Med.* **6**, 245ra95 (2014).

Science Translational Medicine AAAS

www.sciencetranslationalmedicine.org/cgi/content/full/6/245/245ra95/DC1

Supplementary Materials for

An annexin A1–FPR1 interaction contributes to necroptosis of keratinocytes in severe cutaneous adverse drug reactions

Nao Saito, Hongjiang Qiao, Teruki Yanagi, Satoru Shinkuma, Keiko Nishimura, Asuka Suto, Yasuyuki Fujita, Shotaro Suzuki, Toshifumi Nomura, Hideki Nakamura, Koji Nagao, Chikashi Obuse, Hiroshi Shimizu,* Riichiro Abe*

*Corresponding author. E-mail: aberi@med.hokudai.ac.jp (R.A.); shimizu@med.hokudai.ac.jp (H.S.)

Published 16 July 2014, *Sci. Transl. Med.* **6**, 245ra95 (2014)
DOI: 10.1126/scitranslmed.3008227

The PDF file includes:

Fig. S1. Causative drug–specific lymphocytes in patients' peripheral blood.
Fig. S2. The cytotoxicity of supernatant from DIHS/DRESS PBMCs.
Fig. S3. The cytotoxicity of supernatant from irrelevant drug–exposed SJS/TEN PBMCs.
Fig. S4. The cytotoxicity of keratinocytes from normal-appearing postlesional skin and nonlesional skin.
Fig. S5. Protein levels of necroptosis signaling molecules in keratinocytes from SJS/TEN patients, ODSR patients, or healthy controls.
Fig. S6. Effect of poly(I:C), TNF-α, and granulysin on SJS/TEN keratinocyte cytotoxicity.
Fig. S7. The cytotoxicity of $CD14^{bright}$ $CD16^{-}$ and $CD14^{dim}$ $CD16^{+}$ cells on SJS/TEN keratinocytes.
Fig. S8. FPR1 stimulation does not induce phosphorylation of JNK, p38, or ERK.
Fig. S9. Cytotoxicity in SJS/TEN keratinocytes, ODSR keratinocytes, or healthy control keratinocytes induced by PBMC supernatant, as measured by LDH assay.
Table S1. Mass spectrometry result of the proteins in SJS/TEN supernatant.
Table S2. Patient and healthy control information.
Data File S1. The promoter region of FPR1 has no pathogenic mutations.
Reference (*31*)

Supplementary Materials

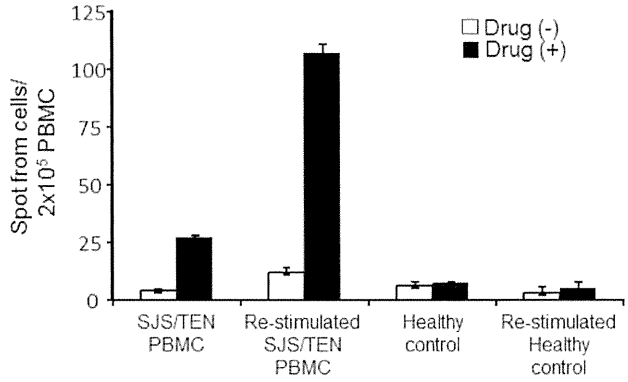

Fig. S1. Causative drug–specific lymphocytes in patients' peripheral blood. Causative drug--specific cells were detected by human IFN-γ ELISPOT. SJS/TEN PBMC, PBMCs from patients who had recovered from SJS/TEN; Re-stimulated SJS/TEN PBMC, PBMCs from patients who had recovered from SJS/TEN that had been cultured with causative drugs for 5 days to proliferate drug-specific T cells. PBMCs were obtained from patient No. 2 and healthy control No. 2.

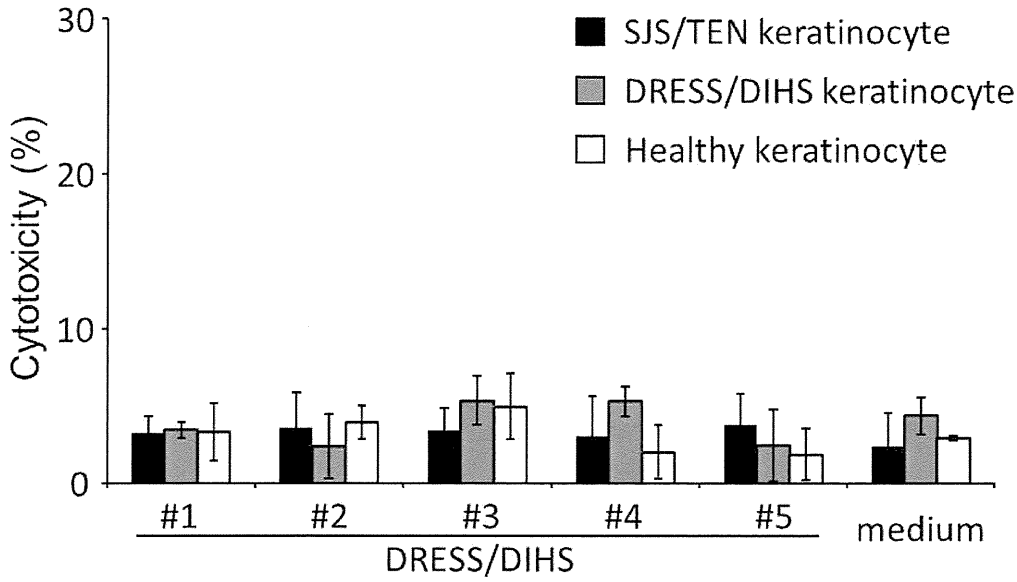

Fig. S2. The cytotoxicity of supernatant from DIHS/DRESS PBMCs. We analyzed the cytotoxicity of supernatants from five DRESS/DIHS patients. The causative drugs were lamotrigine (#1), carpamazepin (#2 and #5), sulfamethoxazole and trimethoprim (#3 and #4). Keratinocytes were obtained from patients No. 5 (SJS/TEN) and No. 22 (DRESS/DIHS) and healthy control No.1. PBMCs were obtained from patients No. 22 (#1), No. 23 (#2), No. 24 (#3), No. 25 (#4) and No. 26 (#5) in Table S2.

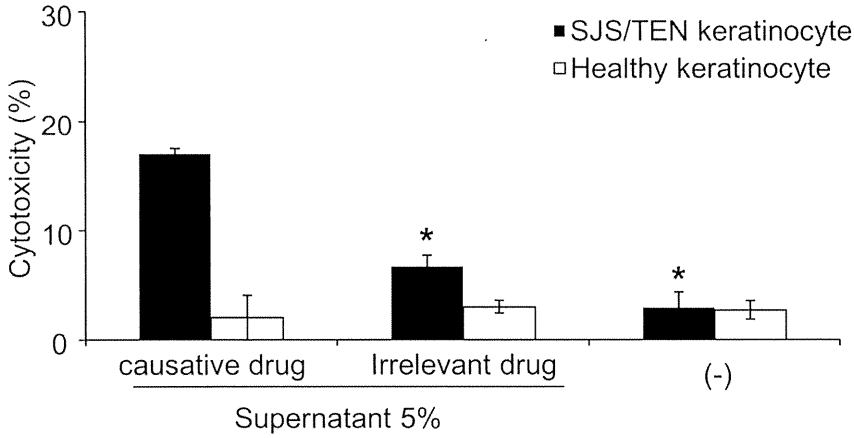

Fig. S3. The cytotoxicity of supernatant from irrelevant drug–exposed SJS/TEN PBMCs.

The cytotoxicity of supernatants from PBMCs stimulated with an irrelevant drug (amoxicillin) were tested. *$P < 0.01$. Keratinocytes were obtained from patient No. 5 (non-lesional skin) and healthy control No.9. PBMCs were obtained from patient No. 5.

A

B

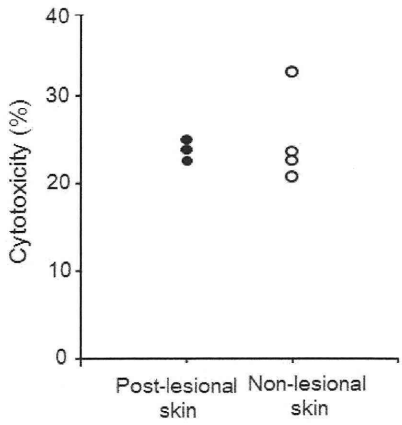

Fig. S4. The cytotoxicity of keratinocytes from normal-appearing postlesional skin and nonlesional skin. (**A**) Photographs of lesional and nonlesional skin. Skin biopsies from SJS/TEN patients were obtained from normal-appearing skin that was lesional during the acute detachment phase but that had returned to normal (postlesional skin), and from normal-appearing non-lesional skin (nonlesional skin). (**B**) Cytotoxicity induced by supernatant from PBMCs of SJS/TEN PBMCs in cultured keratinocytes from normal-appearing postlesional skin and nonlesional skin. Postlesional skin (n=3, patients No. 1, No. 3, No. 10); normal-appearing skin that was nonlesional (nonlesional skin)(n=4, patients No. 4, No. 5, No. 8, No. 9) . Each point